Available online at www.sciencedirect.com
SCIENCE DIRECT®
ELSEVIER
European Journal of Mechanics B/Fluids 23 (2004) 535–550
EUROPEAN JOURNAL OF MECHANICS B/FLUIDS

Turbulence structure in the vortex formation region behind a circular cylinder in lock-on conditions ☆

Alicja Jarża *, Maciej Podolski

Institute of Thermal Machinery, Częstochowa University of Technology, Poland

Received 25 March 2003; received in revised form 8 October 2003; accepted 30 October 2003

Abstract

The present experimental research has been undertaken in order to explain to what extent the turbulent structure of the flow around a stationary rigid cylinder may be affected by an oscillating approach flow. The general aim was to establish a direct link between the oscillating inflow, local time-resolved quantities like skin friction and surface pressure and near wake behaviour behind the circular cylinder. It has been confirmed that the lock-on synchronization between the periodicity of vortex shedding and free stream oscillations is an important factor affecting the formation mechanisms of the wake. In particular it was found that periodical inflow disturbances bring about a rapid growth of pressure and wall shear stress fluctuations near the separation point. The present results revealed also a tendency toward the shortening of vortex formation length and significant growth of the time and linear microscales of turbulence in lock-on conditions. Additional evidence concerning the role of inflow periodical disturbances in the near wake modification was obtained from analysis of turbulent kinetic energy transport in the flow.
© 2003 Elsevier SAS. All rights reserved.

1. Introduction

Flow past bluff cylinders is an important flow type that occurs in many engineering applications. Cylindrical structures exposed to the flow are basically present in all areas of engineering and in the environment. The flow is associated with unsteady vortex shedding and this special feature has a dominant influence on the flow behaviour itself, on the loading of cylindrical structures, which is often unsteady. A wide variety of configurations is possible ranging from infinitely long cylinders in uniform approach flow to the cylinder in shear inflow like boundary layers, cylinders oblique to the approach flow, various cross-sectional geometry, cylinder having short aspect ratios, etc.

In the present paper attention is focused on the long rigid stationary circular cylinder exposed to an oscillatory incident flow. This configuration has many applications in industrial processes. The topic is of direct relevance with regard to offshore platforms, pipelines immersed in waves, heat exchangers, power cables and civil engineering structures in oscillating wind flow. Studies relevant to industrial failures and solutions proposed for design improvement confirm the aerodynamic origin of the problem and are linked to fundamental work in fluid dynamics.

The instantaneous flow in the near wake can be viewed formally [1] as a combination of a mean component $\overline{S}$, a periodic $\tilde{s}$ and a random turbulent s' component, where S is any variable. By definition, the total instantaneous variable S can be expressed as a triple decomposition:

$$S(t) = \overline{S} + \tilde{s}(t) + s'(t). \tag{1}$$

☆ This paper has been supported by the State Committee for Scientific Research, Warsaw, Poland, under statutory funds.
* Corresponding author.
E-mail address: imc@imc.pcz.czest.pl (A. Jarża).

0997-7546/$ – see front matter © 2003 Elsevier SAS. All rights reserved.
doi:10.1016/j.euromechflu.2003.10.017

Nomenclature

b_{05}	half-width of the wake
C_D	drag coefficient
$C_p = 2(p - p_0)/(\rho \overline{U}_0^2)$	surface pressure coefficient
C_{pb}	base pressure coefficient
c'_p	coefficient of pressure fluctuations
d	cylinder diameter
f_0	frequency of the inlet flow disturbances
f_s	vortex shedding frequency
f_{s0}	Strouhal frequency of a stationary cylinder in a uniform incident flow
$\overline{q^2} = \overline{u'_i u'_i}/2$	turbulent kinetic energy
Sh	Strouhal number
$U(t)$	instantaneous flow velocity
$u'_i,\ \tilde{u}_i$	random and periodic velocity fluctuations components
$\overline{U}_i$	time mean velocity
$\overline{U}_0$	mean velocity of the incident flow
ΔU_m	maximum depth of the mean velocity
x_i	coordinate axis, defined in Fig. 1
α	fractional circulation remaining (α_0 – steady inflow, α_s – oscillating approach)
Γ	circulation shed from a body (Γ_0 – steady inflow, Γ_{ms} – oscillating approach)
Θ	angular coordinate of the position around cylinder
$\bar{\tau}_w$	mean wall shear stress
τ'_w	wall shear stress fluctuating component
τ_{11}	longitudinal time micro-scale
λ_{11}	longitudinal linear micro-scale

Symbols

$(\bar{\ })$	time averaged value
$(\tilde{\ })$	oscillating component
$(')$	random component

The oscillating flow field component is a direct result of an alternate vortex generation and shedding into the body wake. On the other hand the organized time-dependent fluctuations of the flow surrounding the bluff body can be introduced through the periodical external disturbances. The experimental work done till now on cylinders in wind tunnels has revealed the important role played by lock-on synchronisation of the vortex shedding and external periodical disturbances. Locking-on was first studied on self-induced oscillations of lightly damped cylinders [2,3]. In order to better understand the factors which influence the lock-on phenomenon, investigations in the last two decades focused on the case of a cylinder forced to oscillate in uniform flow. Tanida et al. [4] showed evidence of locking-on due to cross stream and in-line vibrations of the cylinder. The works concerned with vortex shedding from oscillating bluff cylinders have been reviewed by Sarpkaya [5] and Bearman et al. [6,7]. According to a review given by Griffin and Hall [8] the phenomenon of vortex shedding resonance or lock-on is also observed in the case of a stationary rigid bluff body placed in an oscillatory incident flow. It occurs when the incident velocity field $U_0(t)$ has a periodical component characterized by properly matched frequency f_0 and amplitude A. This opinion agrees well with the results of Armstrong et al. [9,10], Castro [11], Barbi et al. [12], Jarża et al. [13–16]. There is an equivalence between this case and in-line oscillations of the cylinder when the acoustic wavelength is long compared to the cylinder's diameter [8]. Coupling between the mechanism of the Karman vortex street and in-line cylinder vibrations or free stream oscillations occurs near twice the Strouhal frequency. All of these external discrete oscillations, as for example vibrations of the body itself [17] or oscillations of the incident stream are potential means for active control of the near-wake flow behind the bluff body.

In the majority of contributions to the flow over a circular cylinder in the presence of external disturbances only global characteristics are reported, such as the range of amplitudes and frequencies for which lock-on is possible, base pressure, vortex shedding frequency or forces exerted on the cylinder. A region which has so far been overlooked is the immediate neighbourhood of the cylinder where the flow combines random characteristics with some form of organisation. Little is known about local, time resolved wall quantities over a circular cylinder immersed in pulsating streams.

The present experimental research has been undertaken in order to explain to what extent the turbulent structure of the two-dimensional wake-flow may be affected by the incident flow oscillations. Special attention is focused on the organisation of the vortex formation region in lock-on conditions. The unsteady flow field is analysed on the basis of a complete set of mean velocity profiles, Reynolds and coherent stress components and spectral records in the near-wake region. A matter of interest of the present study has also been related to mean and random surface pressure components and wall shear stress evolution around a rigid circular cylinder in oscillatory inflow (Fig. 1). The effect of incident flow periodicity with respect to time and linear scales of turbulence as well as to convective transport of the turbulent energy in the near-wake region has been analysed as a potential means of the wake formation mechanism control.

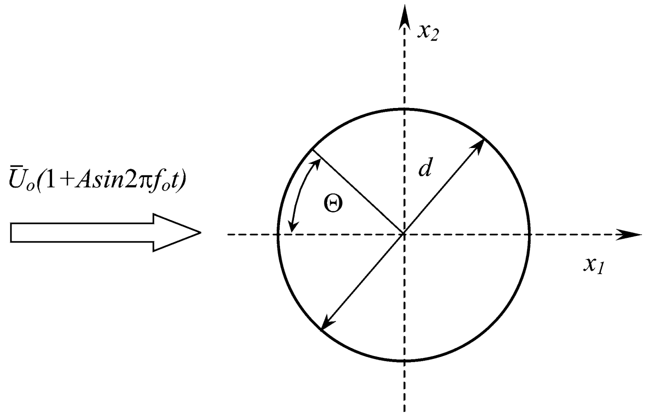

Fig. 1. Schematic sketch of the flow considered.

2. Experimental arrangement

The investigations were carried out in an open-circuit wind tunnel at the Institute of Thermal Machinery of the Częstochowa University of Technology. The test section was (0.6×0.6) m $(W \times H)$ and $\approx$4 m long. The free-stream turbulence did not exceed 0.15% at speeds up to 10 m/s. The circular cylinder of 0.08 m in diameter and 0.6 m long was positioned 1.5 m from the entrance to the working section, perpendicular to the free-stream direction. Thus the geometry of the body-wind tunnel system was determined by the values of two characteristic parameters: aspect ratio $L/d = 7.5$ and tunnel blockage $B = 13\%$.

According to recent reviews, e.g., by Williamson [18,19], the wake of a bluff body is exceedingly rich in three-dimensional vortex dynamics phenomena. So, at any given Reynolds number, the changes of geometrical parameters such as aspect ratio, end constrains and wind tunnel blockage can affect the flow pattern significantly. The effects of end boundary conditions, influencing the flow over the cylinder span should be taken into account if one assumes parallel shedding and 2D-conditions in the mid-span region of cylinder. For the short cylinders, parallel shedding ensues only with the end control techniques. Taking into account the systematic studies by West and Apelt [20,21] the optimised end plates of the Stansby design were used in the present experiment. As a result, the flow around mid-span was effectively decoupled from the end effects except in the region extending approximately 1.5d from each end plate. No attempt at blockage correction has been made in the experiment presented here referring to the results of Cheung and Melbourne [22], and Norberg [23] obtained in similar blockage and aspect ratios conditions.

The controlled oscillations of the incident flow were introduced by means of the set of two shutters rotating in phase at the downstream end of the wind tunnel measuring section. For a schematic of the arrangement see Fig. 2. The generated velocity perturbations were periodic with the fundamental frequency f_0, corresponding to the angular velocity of the shutters ($f_0 = 2n_0$). The checking measurement taken by means of the X hot-wire probe confirmed that the periodical oscillations induced in the measuring chamber had strongly dominating streamwise component superimposed upon the mean fluid motion. The inflow velocity oscillations were nearly sinusoidal, with at least 93% of the pulsation energy at the fundamental frequency. The oscillation amplitude A was kept at the level 7% of the mean flow velocity $\overline{U}_0$. The oncoming stream was thus approximately given by

$$U = \overline{U}_0(1 + A \sin 2\pi f_0 t), \tag{2}$$

where f_0 is the driving frequency. It was checked by means of two pressure transducers on the wind tunnel wall that there was no phase lag between the two corresponding signals, thus confirming the absence of standing acoustic waves.

The complex flow field around the cylinder was studied using the multichannel DISA 55M CTA System with X hot-wire and hot-film probes. Some limitations of hot-wire measurement technique in turbulent near wake flow should be emphasised here. The relatively strong effect of binormal cooling due to the organized inwards/outwards motions in the near wake, high velocity vector angles of attack, coupled with low streamwise velocity values make the hot-wire measurements in this region extremely difficult. In the present experiment an X-array probe provided detailed streamwise and lateral velocity component statistics. To obtain a validation of the X-array probe measurement, which of necessity assume a two-dimensional flow field, additional tests were performed along the wake centreline with a 4-sensor probe.

The skin friction gauge (DISA hot-film probe type 55R47) was flush mounted on the cylinder surface. This probe has been used to measure instantaneous values of shear stress on the wall. The cylinder was rotated by a stepping motor to allow proper orientation of the sensors and measurements at different angular positions. A method of signal processing based on the phase

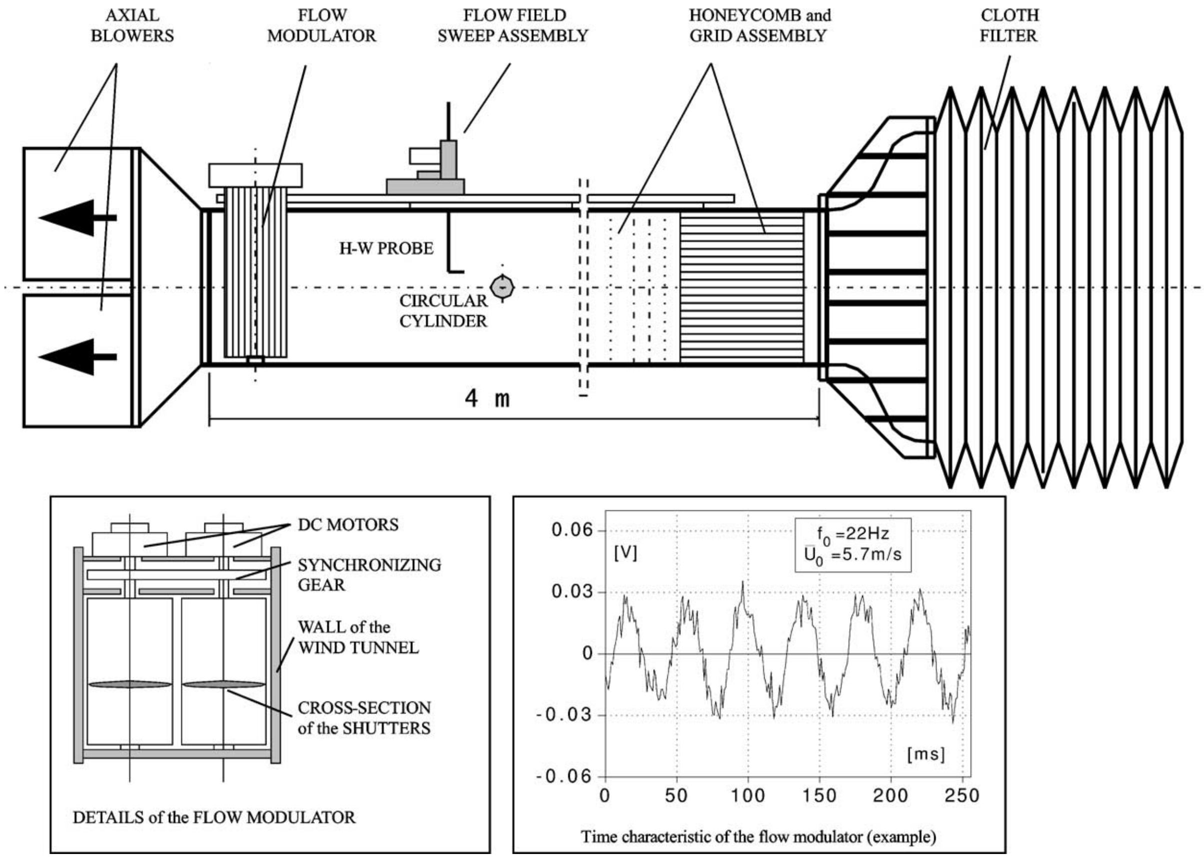

Fig. 2. The scheme of the experimental facility.

averaging technique was applied. The instantaneous pressure signals were transmitted from taps at the surface of the cylinder to the Honeywell pressure transducer type 162PC01D mounted inside the model. Throughout the range of measurement, the output of the pressure probe was linear and the tubing resonant frequency was well above the frequency range investigated.

3. Conditions of the lock-on occurrence

The recognition of the inlet conditions which make it possible to study the vortex lock-on in the context of the active flow control around the circular cylinder is of great importance in the undertaken experimental work. A result of the studies mentioned earlier (Armstrong et al. [9,10], Griffin and Hall [8], Jarża et al. [13–16]) is that the limits of lock-on occurrence can be characterized by a group of mutually related features, which consists of the amplitude A and frequency f_0 of external disturbances and the bluff body natural shedding frequency f_{s0}. The process of synchronisation of periodical events in the flow around the cylinder in oscillating inflow can be detected on the basis of a relation describing the variation of vortex-shedding frequency versus reduced incident velocity for the range of f_0 considered (Fig. 3). In the present experiment, the vortex shedding frequency was determined from power spectra of surface pressure fluctuations recorded near the separation point at the cylinder wall. Sample results of spectral analysis are shown in Fig. 4. The inverse of the Strouhal number, formed using driving frequency f_0 and mean velocity $\overline{U}_0$ is plotted versus f_s/f_0 in Fig. 3. The slope of the line drawn here is a constant equal to 0.197 and it represents the Strouhal number Sh_0 for the Karman vortex street in the case of steady inflow. The locking phenomenon occurs as a plateau near $f_s/f_0 = 0.5$. It means that the over a range of reduced velocity $\overline{U}_0/f_0 d$ the vortex shedding frequency remains at half of the inlet oscillation frequency.

According to present data shown in Fig. 3, the ratio f_s/f_0 is kept constant over a relatively wide range of inlet conditions. For the constant inflow velocity $\overline{U}_0 = 5.7$ m/s lock-on occurrence is limited to the range of driving frequency $f_0 = 22$–28 Hz. Out of this range the vortex shedding frequency tends again to the steady inflow value f_{s0}. One can also estimate the reduced amplitude of the incident oscillations, defined after Barbi et al. [12] as $\varepsilon = A/\pi f_0 d$, where A is “peak-to-peak” inflow

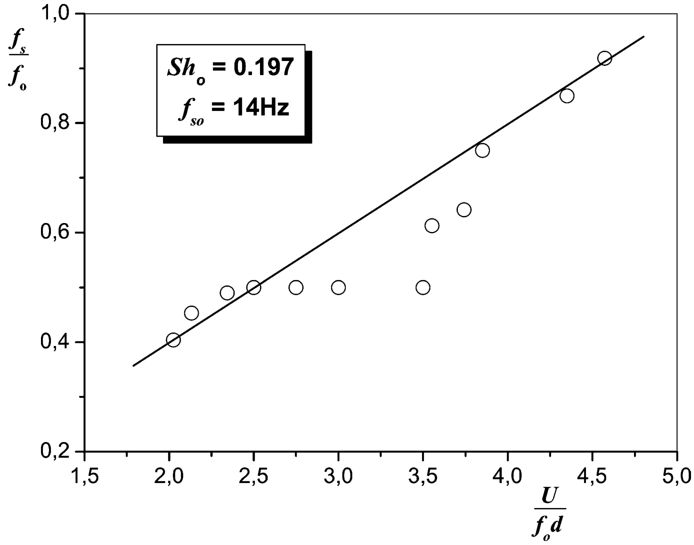

Fig. 3. Vortex shedding frequency versus reduced inflow velocity for the range of f_0 considered.

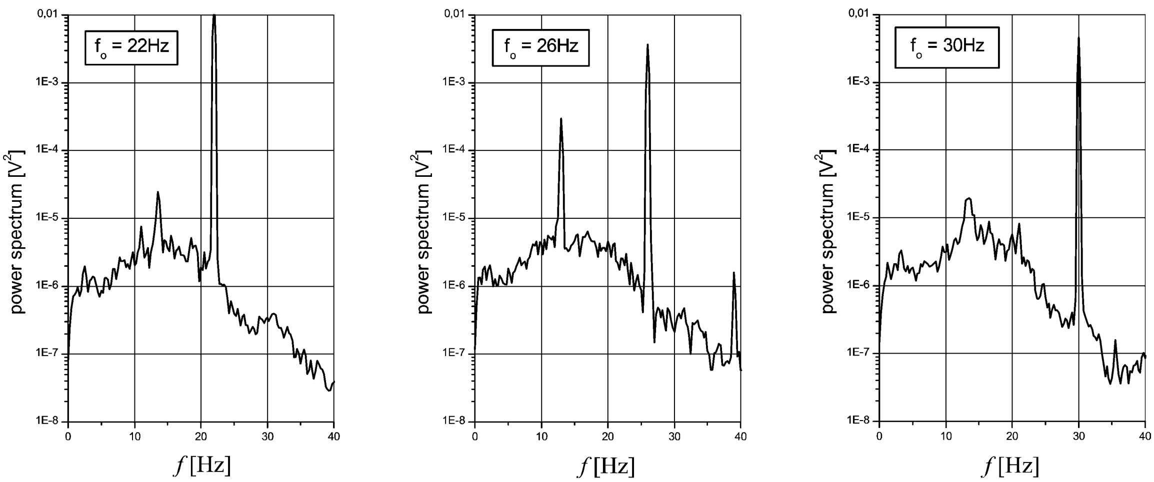

Fig. 4. Sample power spectra of pressure fluctuations at cylinder wall for different values of f_0.

periodicity amplitude. The values of this parameter $\varepsilon = 0.025$–0.11 correspond to the experimental conditions of the earlier investigations of Barbi et al. [12] and Armstrong et al. [9,10], reaching the bounds of lock-on regime.

4. Experimental results and discussion

The present contribution concentrates on the structure of the near wake, which together with the flow properties in the immediate vicinity of the cylinder wall combines random characteristics with a periodical form of organisation. The general aim is to establish direct links between the parameters of inflow periodicity, local time-resolved wall quantities like skin friction and surface pressure and near wake behaviour.

4.1. Measurements at the cylinder wall

Mean pressures around the cylinder surface were measured for a range of parameters of incident flow oscillations and presented as pressure coefficients. Fig. 5 shows a selection of pressure distributions taken in lock-on conditions together with results for steady inflow and out of lock-on region. In the frontal part of the cylinder the normalized pressure is nearly

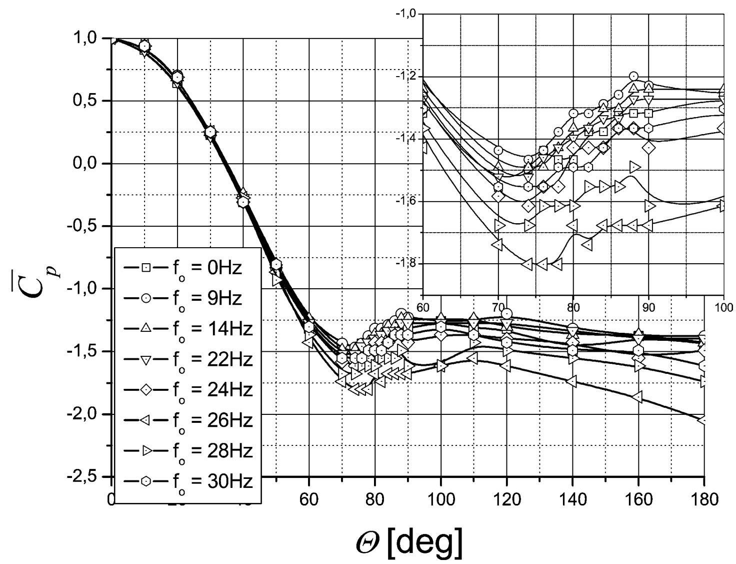

Fig. 5. Distribution of the mean pressure coefficient around the cylinder wall in periodical inflow.

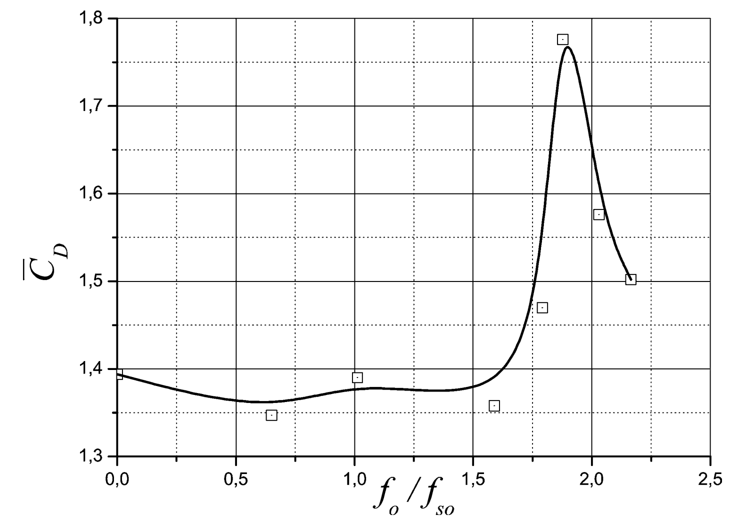

Fig. 6. Effect of incident flow oscillations on the mean drag coefficient.

independent of the inflow conditions. Important changes however are found in the rear as was to be expected. The influence of the external flow oscillations appears to be limited to reducing the pressure coefficient at angular positions larger than 60°. In particular the pressure distributions on the back of the object reveal the changes in base pressure p_{b}, which provides a further useful parameter for identifying the nature of the effects caused by upstream disturbances. The vortex lock-on in the perturbed flow exhibits a particularly strong form of resonance, producing a reduction in base pressure from $C_{\mathrm{pb}} = -1.38$ to -2.05. As a direct result of base pressure changes under inflow oscillations one can observe in Fig. 6 the variation of the drag coefficient, which increases strongly from nearly 1.35 for the uniform incident to 1.75 in lock-on conditions. The experimental quantities mentioned above and describing the flow around the cylinder form a linear relation, common for a wide variety of inflow frequencies. The results shown in Fig. 7 are in good agreement with previous measurements of Surry [24] for steady incident conditions.

All the changes of the flow features in the close vicinity of the cylinder surface should be analysed as a complex phenomena with important role played by vortex shedding and formation. For the understanding of the shear flows over solid walls in the thin region next to the surface, the knowledge of the wall shear stress is very important. From the measurement of the skin friction the information about the position of the separation points, separation bubbles or transition points can be derived.

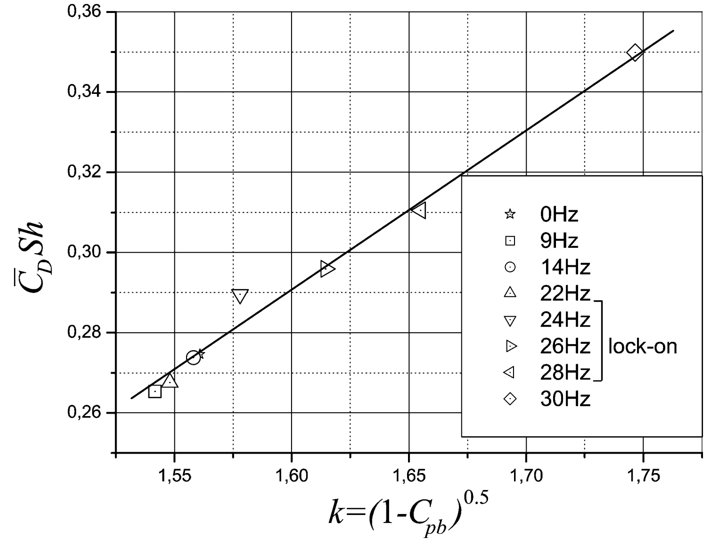

Fig. 7. Relation of the basic aerodynamic parameters.

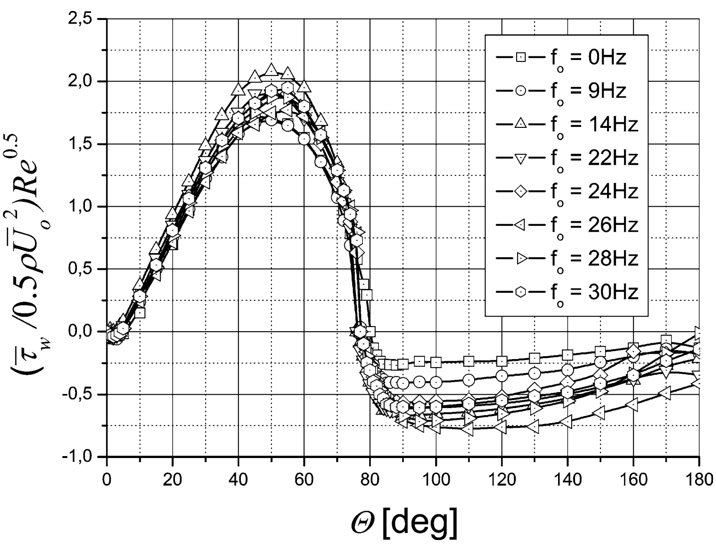

Fig. 8. Normalized values of the mean skin friction at different angular positions in oscillating inflow.

Averaged skin friction distributions presented in normalized form in Fig. 8 revealed a well-known behaviour in the attached region [25]. The skin friction starts from zero at the stagnation point, peaks at about 50°, drops from then on and achieves its negative values in the separation region. There is some increase of absolute skin friction values if the incident flow is oscillating. The separation is indicated by the vanishing of the skin friction. The results just discussed, combined in one diagram in Fig. 8, show a sharp decrease towards the value of zero near $\Theta = 78°–80°$. It appears that data for both steady and oscillating flow collapse in this region. In the present experiment pressure transducers (HONEYWELL) and skin-friction gauges (DISA) were also used to record the fluctuating pressure and skin friction random component, respectively. Fluctuating pressures are presented in the paper as pressure coefficients c'_{p} defined as $2p'_{\mathrm{rms}}/\rho\overline{U}_0^2$, where p'_{rms} is the root-mean-square value of the pressure fluctuations.

The mutual relation between the mean wall shear stress, skin friction fluctuations and surface pressure fluctuations coefficient is shown in Fig. 9(a)–(c). It is interesting to compare Fig. 9(a)–(c) distributions for steady inflow (Fig. 9(a)) with data obtained in pulsating flow both in the lock-on regime (Fig. 9(b)) and out of this condition (Fig. 9(c)). For the case $f_0 = 0$ the general form of the pressure fluctuation distributions stays in accordance with the data of West and Apelt [20]. The occurrence of a maximum of c'_{p} in the vicinity of separation as well as second maximum near $\Theta = 140°$ associated with the vortex formation and shedding is also consistent with description of Achenbach [25]. Periodic inflow disturbances bring about more intensive surface pressure and skin friction fluctuations (see different scales for c_p' in Fig. 9(a) and Figs. 9(b), (c)). One can see the rapid growth of pressure and wall shear stress fluctuations near the separation point indicated by a zero value of mean shear stress. The changes in boundary layer evolution around cylinder are especially visible in the lock-on regime.

In the zone of the highest values of τ_w' and c_p' the distributions of the wall shear stress and pressure fluctuations do not form a distinct peak but embrace some range of angular positions associated with the separation process. One may conclude that the location of separation is changeable in time and space, undergoing oscillations around the position indicated by the zero value of mean skin friction coefficient. In the lock-on conditions the separation process is concentrated in the narrow but distinctly marked range of angles Θ. It should be also emphasised that in the separated region, considered sometimes to be "dead", the level of skin friction fluctuations increases, reaching near $\Theta = 180°$ values as high as in the attached flow region.

The phenomena observed in the immediate neighbourhood of the cylinder wall under influence of inflow oscillations sheds some light on the organisation of the near wake. These and previous [26,27] results suggest that modification and control of the vortex generation mechanisms may provide a means for making substantial changes in the near-wake vortex pattern.

So, it is interesting to consider the effect of the incident flow oscillations on the amount of circulation which is shed from the cylinder. According to Roshko [28] an estimation of the total circulation shed by the body could be done from the value of the mean base pressure. The mean rate of shedding of circulation from a separation point of a bluff body is given approximately by $k \cdot U_0$ where $k^2 = (1 - C_{pb})$. Hence the circulation $\Gamma_m = \Gamma/(U_0 d)$ shed during the formation of a single vortex is expressed as

$$\Gamma_m = \frac{1}{2}(1 - C_{pb})\frac{U_0}{f_s d}. \tag{3}$$

As discussed by Roshko [28], Davies [29] and Balachandar et al. [30], the strength of vortices discharged into the wake will be substantially less than derived form Eq. (3), because a considerable amount of circulation is cancelled in the near wake by mixing with vorticity of opposite sign from the opposing shear layer. So, only a small part of the shed circulation appears in concentrated form. The fractional circulation remaining can be written as

$$\alpha = \frac{2Sh\Gamma_m}{(1 - C_{pb})}. \tag{4}$$

The ratio of circulation Γ_{ms} shed from a body in oscillating inflow to that shed in steady incident conditions Γ_0 is plotted against f_0/f_{s0} in Fig. 10. This figure demonstrates that the circulation shed per cycle is substantially amplified in the lock-on regime. The fraction of circulation α that survives the vortex formation process increases by 16.5% in lock-on conditions comparing with steady inflow (Fig. 11).

4.2. Characteristics of the near-wake development

The properties of the flow disclosed earlier together with the velocity field characteristics behind the bluff body provide an integral picture of this complex region. The data base for the present considerations can be completed by information obtained by Jarża et al. in earlier contributions [13,14]. The main part of the experimental results presented in [13,14] dealt with the near wake flow region and included the mean flow evolution as well as the turbulent structure described by random and periodical fluctuations components. The unsteady flow field characteristics consisted of a complete set of profiles of measured quantities obtained at different distances x_1/d for selected values of inflow oscillations frequency f_0. During the experiment mentioned above the conditions of lock-on occurrence were fulfilled as well as the state outside the range of resonant synchronisation. The data base provided by the aforementioned contributions [13,14] and represented by sample results in Figs. 12–14 could serve here as a set of information for more complex analysis of the near-wake behaviour. The main finding of the previous experiments of Jarża et al. was to conclude that the inlet periodical disturbances intensify the process of mean velocity field stabilisation (Fig. 12). The substantial influence of incident flow oscillations is also observed with respect to the cross component $\overline{u_2'^2}$ of random motion (Fig. 13) and energy of periodical velocity component (Fig. 14). The lock-on synchronisation brings about significant growth of energy in both the random and periodical motion.

In the present analysis a special emphasis has been put on understanding the role of inflow oscillations in the modification of the vortex formation region. Bloor [31] defines the vortex formation length as the distance behind the cylinder where the maximum level of periodicity of the hot-wire signal is observed near the wake axis. This implies that the end of the formation process coincides with the moment at which the fluid from outside the wake reaches and crosses the axis. The fluid is drawn across the wake by the action of the growing vortex on the other side. As has been noted above (see Figs. 8 and 9) the amount of circulation shed from the cylinder is amplified due to lock-on. The additional vorticity produced reinforces the currently developing vortex and accelerates its growth closer to the rear face of the body.

Thus, one may expect the shortening of the vortex forming distance under lock-on conditions. To verify this spectral analysis of the hot-wire signals has been applied for the probe located at various points in the near wake region. A clearly defined peak at

(a)

(b)

(c)

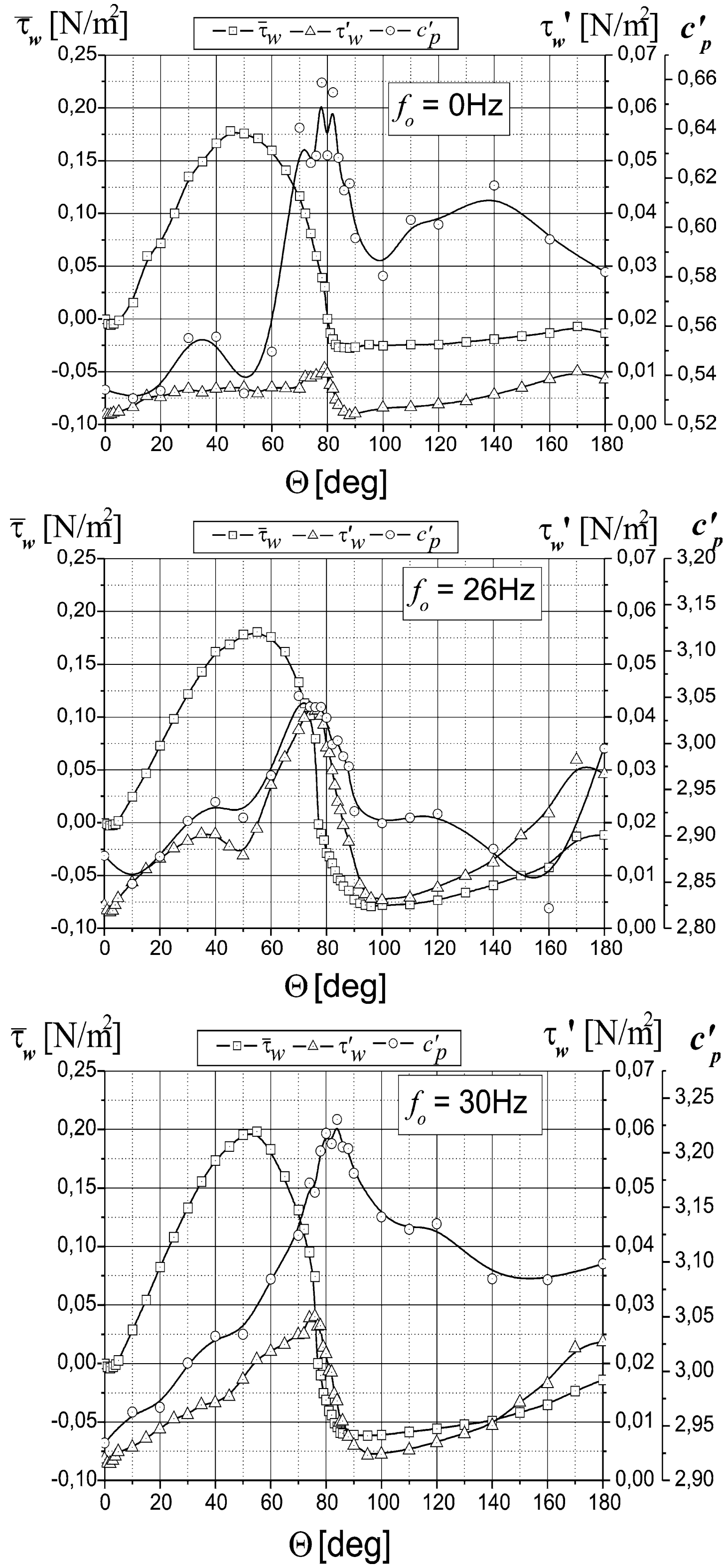

Fig. 9. Distributions of the mean wall shear stress ($\bar{\tau}_\mathrm{w}$), wall shear stress fluctuations (τ'_w) and surface pressure fluctuations coefficient (c'_p) around cylinder in (a) steady ($f_0 = 0$ Hz) and oscillatory inflow for (b) lock-on conditions ($f_0 = 26$ Hz) and (c) out of lock-on range ($f_0 = 30$ Hz).

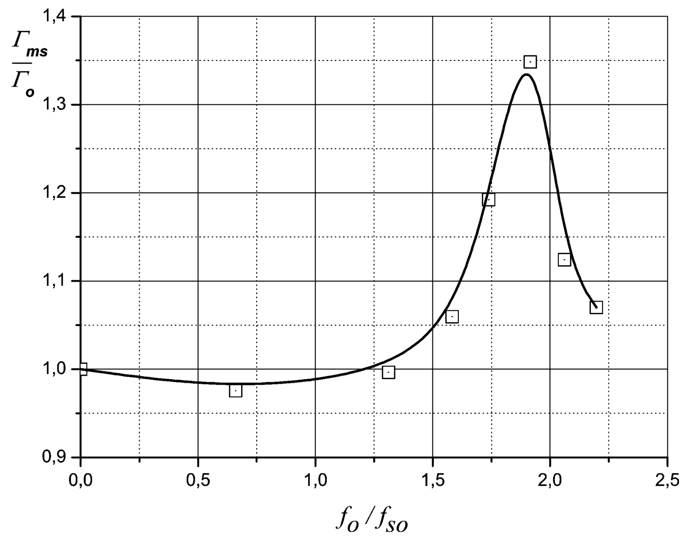

Fig. 10. Amplification of circulation shed from the body in periodical inflow conditions.

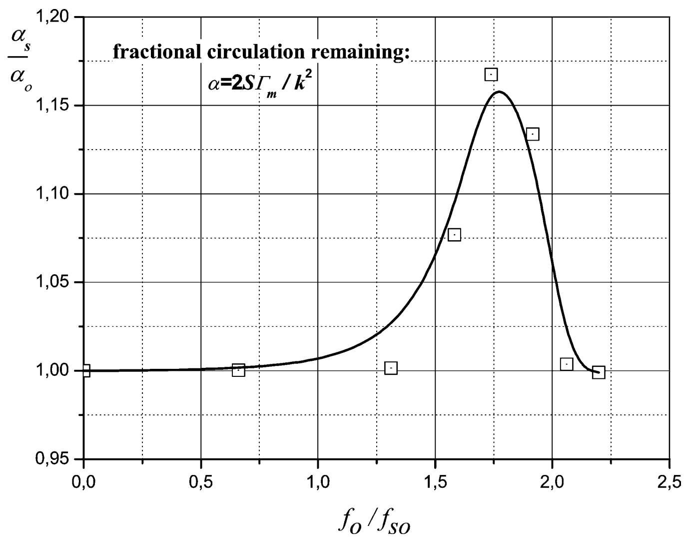

Fig. 11. Ratio of fractional circulation for the oscillating and steady inflow.

the vortex shedding frequency containing the major part of the total energy is an obvious feature of the spectral distributions in the vortex street. The incident flow disturbances change the Strouhal peak amplitude in the velocity fluctuations spectra. These changes have been expressed here by means of the parameter ΔE(Fig. 15). On the basis of distributions presented here for different values of driving frequency f_0 one can estimate the bounds of the vortex formation zone identified by the location of the maximum of ΔE. As can be seen in Fig. 15, the inlet flow oscillations intensify the vortex forming, especially in lock-on conditions.

This can be additionally confirmed by the data set shown before in Fig. 14, presenting the evolution of the kinetic energy component corresponding to oscillating motion. The kinetic energy of oscillations has been expressed here through the averaged values obtained by integrating the profile of $\overline{\tilde{u}_2^2}$ component in a particular cross section $x_1 = const$. The maximum energy level observed in the lock-on state is reached at a short distance behind cylinder, approximately the same as indicated by spectral analysis (see Fig. 15).

The effect of incident stream oscillations has also been observed through the changes of time and linear micro-scales of turbulence estimated by means of auto-correlation analysis of hot-wire signals under the assumption of the Taylor hypothesis [32]. The longitudinal component of velocity fluctuations has been taken into account in the present considerations. It may

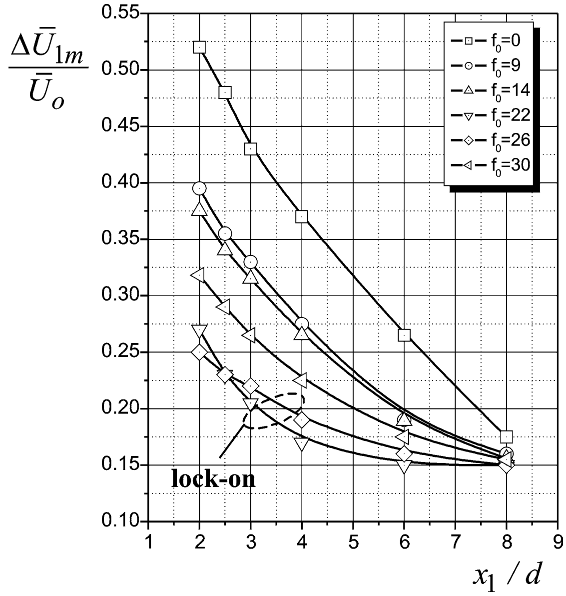

Fig. 12. Decay of nonuniformity parameter of the mean velocity component $\overline{U}_1$.

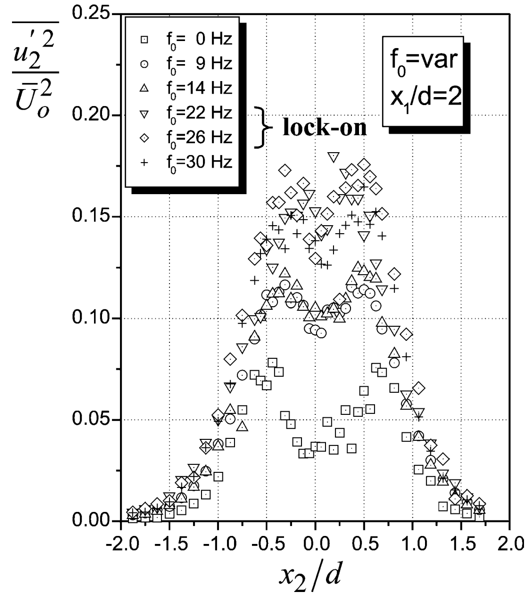

Fig. 13. Sample lateral distributions of the normal turbulent stress component $\overline{u_2'^2}$.

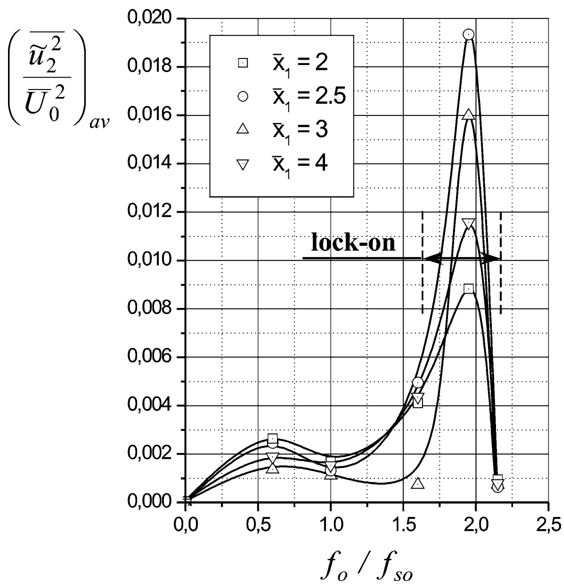

Fig. 14. Effect of lock-on conditions on the average (for the wake cross section $\bar{x}_1 = const$) value of kinetic energy corresponding to oscillating velocity component.

be concluded from Fig. 16 that the mean size λ_{11} of fine vortex structures in the near wake region stays nearly constant in downstream direction. Lock-on brings about significant growth of the vortex size measure λ_{11} visible as a local maximum for the resonance frequencies f_0. The time-microscale τ_{11} (Fig. 17) increases outward from the wake axis, and keeps nearly constant in the flow direction.

An additional evidence concerning the role of inflow periodical disturbances in the near wake modification was obtained from analysis of turbulent kinetic energy distributions. The isolines of total kinetic energy of all the random velocity components ($\overline{q^2} = \overline{u_2'^2}/2$), juxtaposed in Fig. 18 for different values of driving frequency f_0, reveal an essential changes of the turbulent energy levels in the cylinder near-wake under the influence of external periodical disturbances. One can observe here the zones

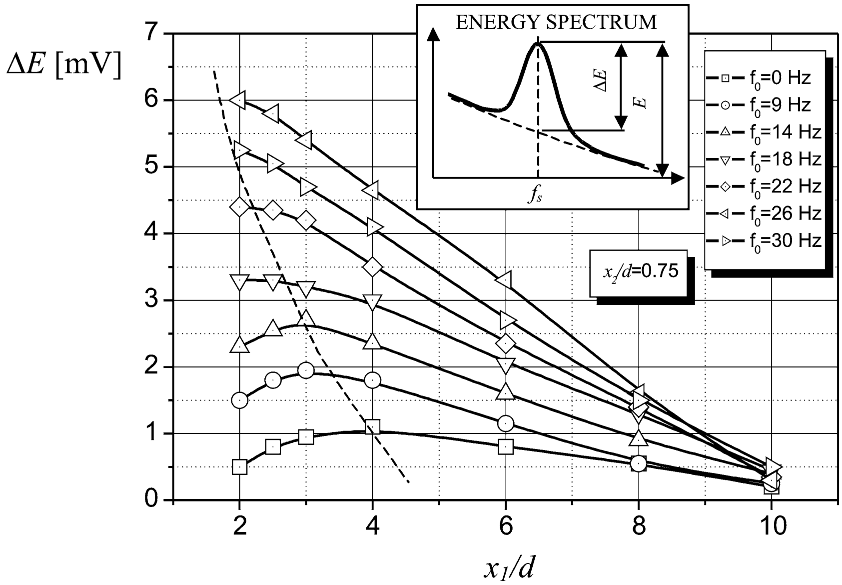

Fig. 15. Changes of Strouhal peak amplitude in velocity fluctuations spectrum for vortex formation zone.

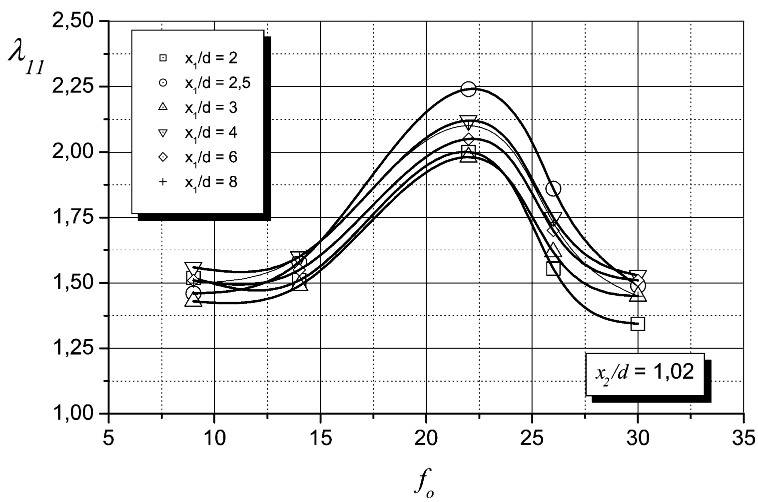

Fig. 16. Linear micro-scale distributions through the near-wake flow in lock-on conditions ($f_0 = 22$ Hz).

of high turbulence energy concentration, appearing in the central part of the wake near the vortex formation distance as the lock-on synchronization is being achieved. The strong kinetic energy gradients in the longitudinal and cross stream directions, which accompany the increase of random velocity fluctuations in the vortex formation zone, decay gradually out of lock-on range.

The turbulent energy distributions discussed here are related with the convection process, which is one of the important mechanisms responsible for the turbulent energy transport in the wake flow. Convection by the mean flow, being a term of the kinetic energy equation [32], can be written as the sum of two energy streams transferred by longitudinal and transverse mean velocity components:

$$CONV = \frac{1}{2}\overline{U}_1\frac{\partial\overline{q^2}}{\partial x_1} + \frac{1}{2}\overline{U}_2\frac{\partial\overline{q^2}}{\partial x_2}.$$

An experimental analysis of the convective component of the turbulence energy budget has been possible on the basis of records of X hot-wire signals taken in the near wake flow region. Sample results of instantaneous signal processing, for the distance $x_1/d = 2$, are shown in Fig. 19, presenting the profiles of turbulence energy streams transported by convection. The values of

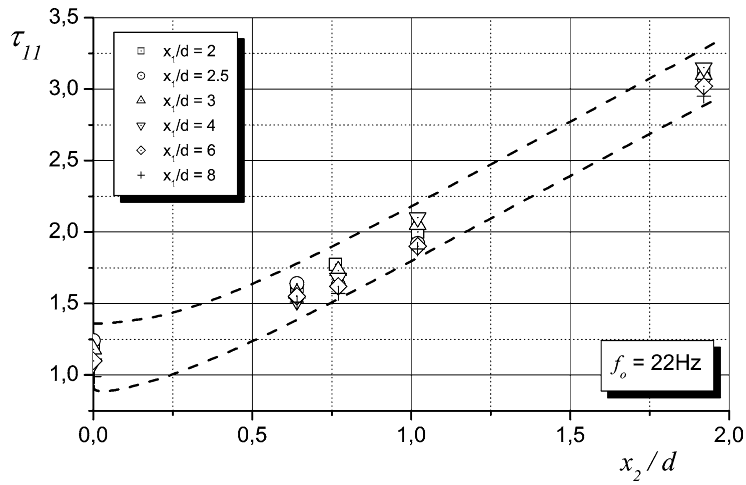

Fig. 17. The effect of inflow oscillations upon the longitudinal time micro-scale of turbulent motion in the wake flow.

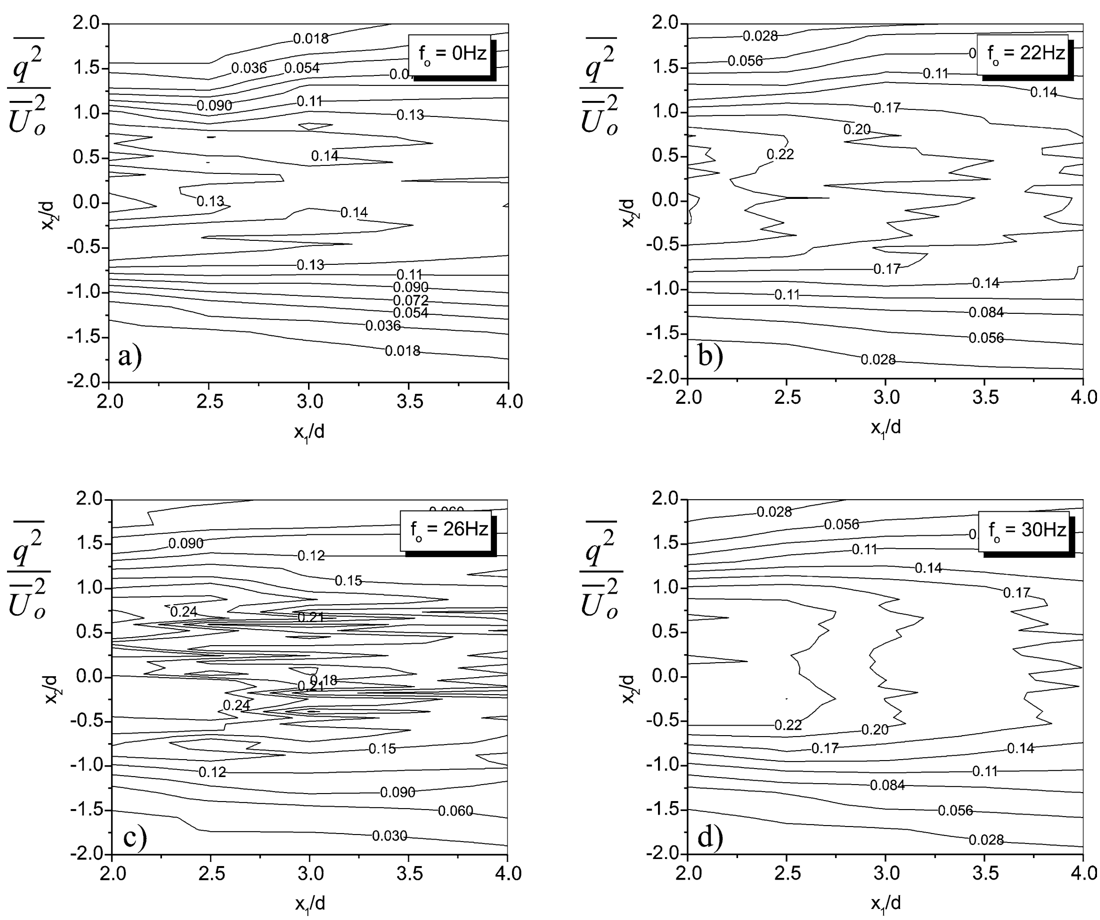

Fig. 18. Isolines of turbulent kinetic energy in near-wake-flow for steady inflow (a) $f_0 = 0$ Hz, lock-on conditions (b) $f_0 = 22$ Hz, (c) $f_0 = 26$ Hz and out of synchronization range (d) $f_0 = 30$ Hz.

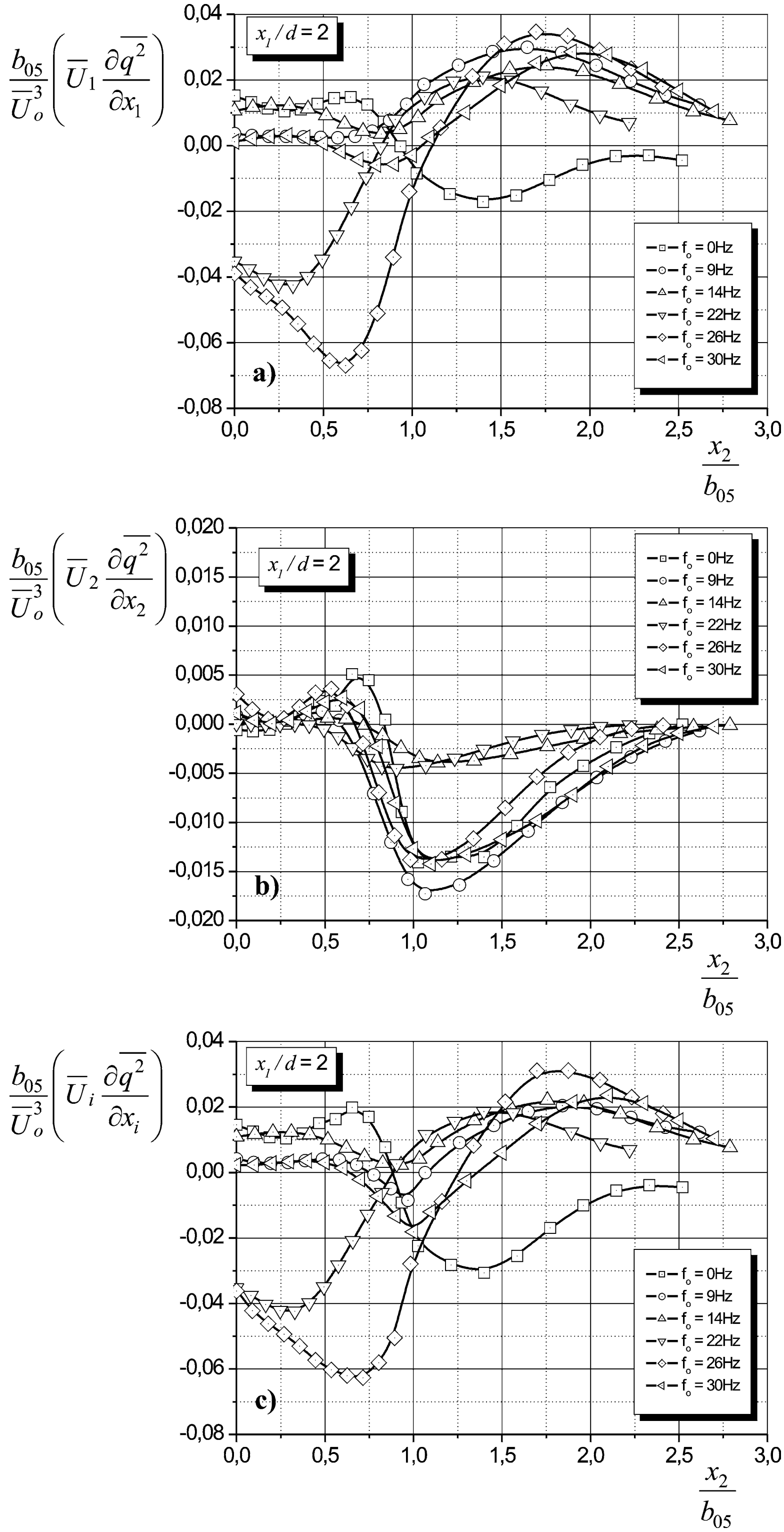

Fig. 19. The effect of inflow oscillations on the lateral distributions of the turbulence energy convection due to longitudinal (a) and cross (b) mean velocity components as well as total convective stream (c) for the distance $x_1/d = 2$ behind the cylinder.

the longitudinal (Fig. 19(a)) and cross stream (Fig. 19(b)) components of the total convection (Fig. 19(c)) have been normalized using the half-width of the wake b_{05} as the characteristic linear measure. The effect of inflow periodicity is clearly visible in the figure with respect to both convection terms considered. One can notice, that the convective transport of turbulent kinetic energy is dominated by the longitudinal stream. The share of convection due to lateral mean velocity component does not change the global picture of the convection process in the very near wake flow region. The distinct changes in the convective stream distributions are especially marked in lock-on conditions ($f_0 = 22$–28 Hz). It should be emphasised first of all, that in the resonant state the convection term changes its sign and reaches high negative values in the central part of the wake. Thus, one can conclude that the convective transport of the random fluctuations' energy into the near axis zone is very intensive and, in consequence, the turbulent kinetic energy concentrates in the middle part of the wake. It is consistant with the previous finding (Fig. 18) about the changes in turbulent energy distributions in the vortex formation region under lock-on influence. The positive values of convection observed in the outer wake region indicate the downstream direction of energy transfer by convection out of the central part of the wake.

5. Concluding remarks

Lock-on synchronization between the periodicity of vortex shedding and free stream oscillations is an important factor affecting the formation mechanisms of the wake. Inflow oscillations have a dominant influence, which can be large even outside the lock-on range. In particular it was found that the periodical inflow disturbances bring about more intensive surface pressure and skin friction fluctuations. A rapid growth of pressure and wall shear stress fluctuations has been noticed near the separation point. The oscillations of the incident flow considerably change the vortex street geometry. Lock-on synchronisation amplifies the eddies characterized by a frequency close to the subharmonic of inlet oscillations. The present results revealed also the tendency toward the shortening of the vortex formation length and significant growth of the time and linear microscales of turbulence in lock-on conditions. Substantial effects are noted also with respect to the distributions of random and periodical fluctuations near the vortex formation distance, where the concentration of the total turbulence energy takes place.

Additional evidence concerning the role of inflow periodical disturbances in the near wake modification was obtained from analysis of the convective transport of turbulent kinetic energy. In lock-on conditions the turbulence energy transport through convection becomes more intense. Its amplification is especially noted in the wake axis region.

Summing up, the present research has confirmed previous suggestions that the vortex forming and turbulence structure in the near-wake-flow can be modified in promising ways through a change of oscillatory inlet conditions.

References

[1] R.J. Adrian, K.T. Christensen, Z.C. Liu, Analysis and interpretation of instantaneous turbulent velocity fields, Exp. Fluid 29 (2000) 275–290.
[2] N. Ferguson, G.V. Parkinson, Surface and wake flow phenomena of the vortex-excited oscillation of a circular cylinder, J. Engrg. Industry Trans. ASME (1967).
[3] D. Rockwell, Vortex-body interactions, Fluid Mech. 30 (1998) 199–229.
[4] Y. Tanida, A. Okajima, Y. Watanabe, Stability of a circular cylinder oscillating in uniform flow or in a wake, J. Fluid Mech. 61 (4) (1973) 769–784.
[5] T. Sarpkaya, Vortex-induced oscillations – a selective review, J. Appl. Mech. 46 (1979) 241–257.
[6] P.W. Bearman, J.M.R. Graham, Vortex shedding from bluff bodies in oscillatory flow: a report on Euromech 119, J. Fluid Mech. 99 (2) (1980) 225–245.
[7] P.W. Bearman, Developments in the understanding of bluff body flows, JSME Int. J. Ser. B 41 (1) (1998).
[8] O.M. Griffin, M.S. Hall, Review – vortex shedding lock-on and flow control in bluff body wakes, J. Fluids Engrg. 113 (1991).
[9] B.J. Armstrong, F.H. Barnes, J. Grant, The effect of a perturbations on the flow over a cylinder, Phys. Fluids 29 (1986) 2095–2102.
[10] B.J. Armstrong, F.H. Barnes, A comparison of the structure of the wake behind a circular cylinder in a steady flow with that in a perturbed flow, Phys. Fluids 30 (1) (1987) 19–26.
[11] I.P. Castro, Vortex shedding from ring in oscillatory flow, J. Wind Engrg. Industr. Aerodynam. 69–71 (1997) 387–398.
[12] C. Barbi, D.P. Favier, C.A. Maresca, D.P. Felionis, Vortex shedding and lock-on of a circular cylinder in oscillatory flow, J. Fluid Mech. 170 (1986) 527–544.
[13] A. Jarża, K. Słomczyński, Vortex shedding from circular cylinder in oscillatory incident flow, J. Theoret. Appl. Mech. 2 (1996) 34.
[14] A. Jarża, T. Tarnowski, Turbulent flow around circular cylinder in oscillatory inlet conditions, Trans. IFFM 105 (1999) 3–16.
[15] A. Jarża, M. Podolski, A study of turbulent transport processes in the near wake of cylinder under controlled inflow oscillations, in: Advances in Turbulence VIII, Proc. of VIII European Turbulence Conference (ETC8), 2000, p. 960.
[16] A. Jarża, M. Podolski, Random and periodical velocity fluctuations in vortex formation region behind cylinder in lock-on regime, in: Proc. of IV IUTAM Symposium on Bluff Body Wakes, Marsylia, 2000.

[17] P.T. Tokumaru, P.E. Dimotakis, Rotary oscillation control of a cylinder wake, J. Fluid Mech. 224 (1991) 77–90.
[18] C.H.K. Williamson, Sinusoidal flow relative to circular cylinder, J. Fluid Mech. 155 (1985) 141–174.
[19] C.H.K. Williamson, Vortex dynamics in the cylinder wake, Fluid Mech. 28 (1996) 477–539.
[20] G.S. West, C.J. Apelt, Measurements of fluctuating pressures and forces on a circular cylinder in the Reynolds number range 10" to 2.5×10^5, J. Fluids Struct. (1993) 227–244.
[21] G.S. West, C.J. Apelt, The effects of tunnel blockage and aspect ratio on the mean flow past a circular cylinder with Reynolds numbers between 104 and 10^5, J. Fluid Mech. 114 (1982) 361–377.
[22] C.K. Cheung, W.H. Melbourne, Turbulence effect on some aerodynamic parameters of a circular cylinder at supercritical Reynolds numbers, J. Wind Engrg. Industr. Aerodynam. 14 (1983) 399–410.
[23] C. Norberg, An experimental investigation of the flow around a circular cylinder: influence of aspect ratio, J. Fluid Mech. 258 (1994) 287–316.
[24] D. Surry, Some effects on intense turbulence on the aerodynamics of a circular cylinder at subcritical Reynolds number, J. Fluid Mech. 52 (3) (1972) 543–563.
[25] E. Achenbach, Distribution of local pressure and skin friction around a circular cylinder in cross-flow up to Re = 5×10^6, J. Fluid Mech. 34 (4) (1968) 625–639.
[26] M.D. Gunzburger, H.C. Lee, Feedback control of Karman vortex shedding, Trans. ASME 63 (1996) 828–835.
[27] D.P. Telionis, M. Gundappa, T.E. Diller, On the organization of the flow and heat transfer in the near wake of a circular cylinder in steady and pulsed flow, Trans. ASME. 114 (1992) 348–355.
[28] A. Roshko, On development of turbulent wakes from vortex streets, NACA Rep. 1191, 1954.
[29] M.E. Davies, A comparison of the wake structure of a stationary and oscillating bluff body, using a conditional averaging technique, J. Fluid Mech. 75 (2) (1976) 209–231.
[30] S. Balachandar, R. Mittal, F.M. Najjar, Properties of the mean recirculation region in the wakes of two-dimensional bluff bodies, J. Fluid Mech. 351 (1997) 167–199.
[31] M.S. Bloor, The transition to turbulence in the wake of a circular cylinder, J. Fluid Mech. 19 (1964) 290.
[32] J.O. Hinze, Turbulence, McGraw-Hill, 1975.